

Hot fragmentation of nuclei*

W. Trautmann^a

^a Gesellschaft für Schwerionenforschung (GSI)
D-64291 Darmstadt, Germany

Today, we have a variety of reactions at hand that can be used to multi-fragment nuclei. In many of these reactions even several sources of fragments can be discerned and characterized.

There is overwhelming evidence that these sources of fragments are hot. It is already less clear whether heat by itself is sufficient to initiate the fragment decay. What causes fragmentation, and when and how are the fragments (pre)formed? These questions have remained as much a challenge as the complementary class of questions to which they are related: What observations derive their significance from the liquid-gas phase behavior of extended nuclear matter? And, can we observe a phase transition in finite nuclei?

Recent developments, largely coming from complex analyses of data sets measured in 4π -type experiments as well as from calculations based on advanced theoretical concepts, will be discussed.

1. INTRODUCTION

Fragmentation is a term commonly used to specify a nuclear disassembly by force. Hot fragmentation is meant to indicate the most violent of these processes, following excitations beyond the limits of nuclear binding, but still ending with bound nuclear fragments of different sizes in the final channels. The formation mechanism of these fragments, whether they are the remnants of an incomplete destruction or the products of a condensation ('selforganization', cf. Ref. [1]) out of the disordered matter, has continued to be the topic of very active research in recent years [2–4].

A two-stage scenario has proven to be fruitful for the interpretation and modelling of hot-fragmentation reactions. It is motivated by the differences of the wave lengths and time scales governing the entrance and exit channels and justified by the remarkable success of statistical approaches for the second stage [5–7]. The intermediate states are not necessarily equivalent to hot nuclei but should be, more generally, viewed as systems of highly excited nuclear matter, populating a phase space characterized by global quantities like mass, charge, energy, density or temperature. Molecular-dynamics calculations can now continuously follow the reaction process from the first encounter to the final disassembly stages without the need to specifically assume equilibration [8–10]. In that sense, they present a challenge to the statistical two-stage picture. On the other hand, the extraction

*Invited Talk at Seventh International Conference on Nucleus-Nucleus Collisions, Strasbourg, France, July 3 - 7, 2000

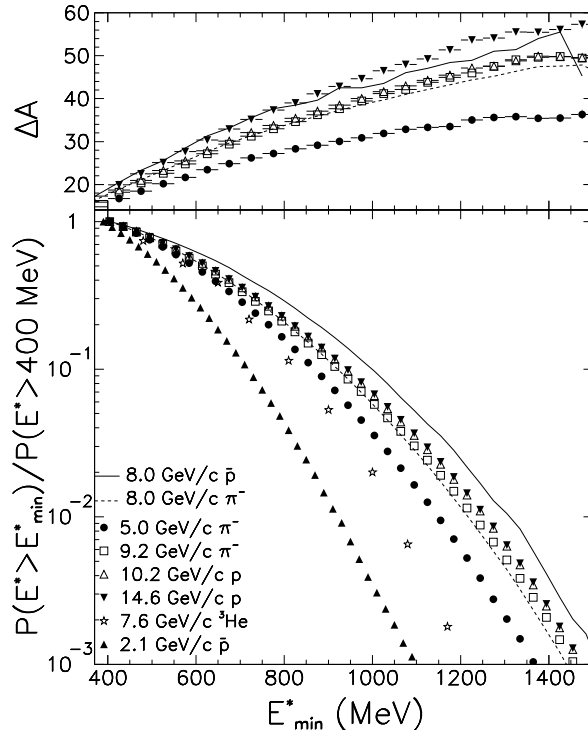


Figure 1. Reactions of energetic hadrons with ^{197}Au targets: average mass loss ΔA in the fast cascade (top) and relative probability for excitation energies $E^* > E_{\text{min}}^*$ (bottom) as a function of E_{min}^* (from Ref. [15]).

of thermodynamical parameters from transport-model calculations has demonstrated that a connection to the statistical approach can be established [11].

There is little doubt that the densities are low and the temperatures high in the intermediate state, coinciding with the values predicted for the coexistence region of liquid and gaseous nuclear matter. To search for observable links of the multifragmentation phenomenon to the predicted phase transition has therefore been a major motivation for many experimental and theoretical activities. It is evident from the titles and abstracts submitted to this conference that there is growing confidence that signals of this phase transition are actually being observed.

This talk divides into three main parts: a brief review of the reactions that are being used to produce hot nuclear systems, a discussion of the caloric curve of nuclei as a potential signature of the liquid-gas phase transition in finite systems, and new experimental results for the conditions at breakup in spectator reactions. This last part will mainly reflect recent activities of the ALADIN collaboration.

2. USEFUL REACTIONS

Thermal fragmentation denotes a concept of studying the breakup of thermally excited nuclear systems formed in collisions of relativistic hadrons with heavy target nuclei. It is

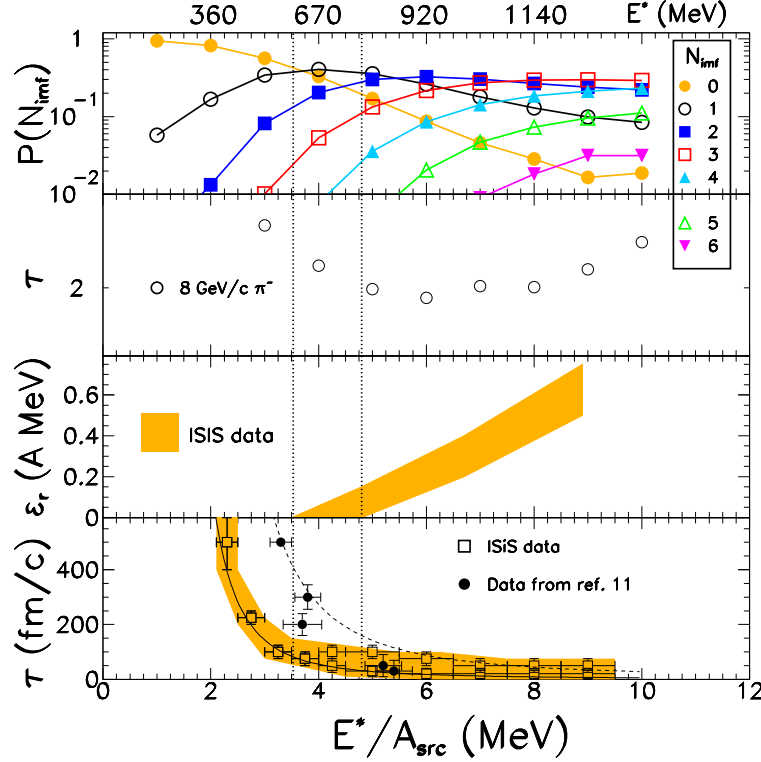


Figure 2. Reactions of energetic hadrons with ^{197}Au targets: distribution of fragment multiplicities N_{imf} , τ parameter describing the element distribution, radial flow energy, and emission time scale (from top to bottom). Ref. 11 in the bottom panel refers to [17] (from Refs. [15,16]).

based on the expectation, tested with intranuclear-cascade calculations, that light energetic projectiles will generate a statistical (thermal) disorder without exciting collective modes such as compression, rotation or shape deformations. The latter are known to break nuclei very efficiently [12,13], and thus would mask the nuclear response to the thermal excitation.

The potential and the limits of this approach have been explored by the ISiS collaboration in their recent experiments at the AGS in Brookhaven with a variety of primary and secondary beams including pions and antiprotons in the momentum range up to 14.6 GeV/c [14–16]. The properties of intermediate systems produced in these reactions are summarized in Fig. 1. Target-like residues with several hundreds of MeV excitation have the largest cross sections, but excitation energies exceeding 1 GeV can be reached, even though with rapidly dropping cross sections. There is also a loss of mass caused by the heating mechanism at relativistic energies. Some of the nucleons participating in the cascading processes are too energetic to remain part of the intermediate system.

The multi-fragment channels open up at the higher excitation energies, as illustrated in Fig. 2. The transition from residue production to hot fragmentation, highlighted by the dotted vertical lines, is, most notably, associated with a striking decrease of the emission

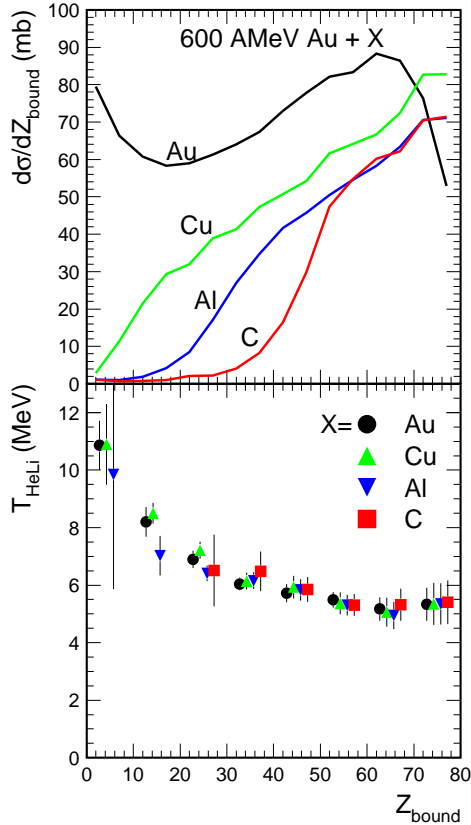


Figure 3. Differential cross section $d\sigma/dZ_{\text{bound}}$ (top) and isotope temperature T_{HeLi} (bottom) as a function of Z_{bound} for the reaction ^{197}Au on Au, Cu, Al and C targets at 600 A MeV. Note that the experimental trigger suppresses the very peripheral collisions at $Z_{\text{bound}} \geq 65$ which have much larger cross sections than indicated here (from Ref. [29]).

time scales to values in the vicinity of 50 fm/c.

According to Fig. 1, the most efficient projectiles are antiprotons of high momentum which only are difficult to use because of their low abundance in the secondary beam [14]. Some extra heating is generated by the pion cascades from the \bar{p} annihilation which leads to considerable excitation energies already at much lower \bar{p} momenta. The reported fragment multiplicities, however, are significantly smaller for the less energetic antiproton beams even if identical bins of excitation energy are selected [18]. It is therefore an open question whether the excitation energy by itself is the only parameter that governs the decay properties and fragment production. Similar questions have recently been raised by other authors who find fewer fragments in the experiment than are predicted by statistical models [19,20]. While this may be partly connected to the difficulties inherent with experimentally determining the thermalized excitation energy [21], it is nevertheless obvious that the solution to this problem will help us to better understand how fragments are formed [22].

The limits of generating excitation energy can be overcome with composite projectiles. Systematic sets of data with projectiles of different mass and energy have been collected by the FASA [23,24], EOS [25–27] and KEK/HIMAC [28] collaborations, and new results are reported in contributions to this conference. The continuing rise of the cross section for high excitations with increasing mass of the collision partner is demonstrated in Fig. 3 for the fragmentation of ^{197}Au projectiles studied by the ALADIN collaboration. These data are shown as a function of the variable Z_{bound} , representing the sum of the atomic

numbers Z_i of all projectile fragments with $Z_i \geq 2$, which is inversely correlated with the excitation energy [21]. As an example of the Z_{bound} scaling, a prominent feature of spectator reactions up to very high energies [30], the isotope temperatures T_{HeLi} are also given in the figure. They are close to 6 MeV for the major part of the Z_{bound} range, but tend to higher values at low Z_{bound} , i.e. at the highest excitation energies reached in these reactions. The temperatures depend only on Z_{bound} but not on the specific target that is used to fragment the ^{197}Au projectile.

Large systems at even higher excitations can be produced in central collisions of heavy systems. In this case, the idea of excitation as a simple heating process has to be abandoned, however. Collective modes, compression as well as the directed outward motion of particles and clusters from primary collisions generate an explosive pattern, quantified as collective radial flow [31]. The production of large clusters is rare and inversely correlated with the observed amount of flow. An extreme case, observed at the AGS, has been reported very recently. For ^{197}Au beams of 11.5 GeV/c per nucleon, centrally colliding with heavy targets, the fragment mass yields are steeply exponential with a penalty factor of about 50 for each additional mass unit [32]. The characteristic transition from power law to exponential spectra, as radial flow sets in [33], has been reproduced with molecular dynamics calculations, very recently e.g. with quantum molecular dynamics [34], but to fully understand the clusterization mechanism in the dynamical environment still remains an interesting problem for future research [1,35].

Heavy symmetric systems below the threshold of collective radial flow (about 50 MeV per nucleon) have been extensively studied by the Miniball/Multics and INDRA collaborations. High-statistics data permit the selection of single-source formation which occurs with small cross sections in central collisions [36,37]. In more peripheral encounters, several sources contribute to the fragment yields with a clear enhancement in the mid-rapidity domain [38]. The potential mechanisms of mid-rapidity emissions, as e.g. neck formation, and the isospin effects associated with it [39,40] are closely connected to several dynamical and statistical aspects of hot fragmentation, among them the isotopic separation expected in the liquid-gas coexistence zone [41–43]. These topics are the subjects of other plenary talks at this conference.

3. LIQUID-GAS PHASE TRANSITION

It is commonly accepted that extended nuclear matter should exhibit a liquid-gas phase transition, following from the Van-der-Waals-like range dependence of the nuclear force [41,44,45]. Sharp discontinuities in the infinite system are expected to broaden as the system size decreases [46,47]. This, however, does not contradict the existence or prevent the identification of phase transitions in small systems with constituent numbers on the nuclear scale [4,48].

The appropriate experiment for identifying the liquid-gas phase transition in finite nuclei has recently been done, theoretically. Fermionic as well as antisymmetrized molecular dynamics (FMD, AMD) models were used to study the equilibrium dynamics of small nuclear systems [49,50]. None of the necessary ingredients were missing in these studies, a container to confine the system, a controllable heating technique, long propagation times to allow the system to settle into equilibrium, and a suitable technique of measuring the

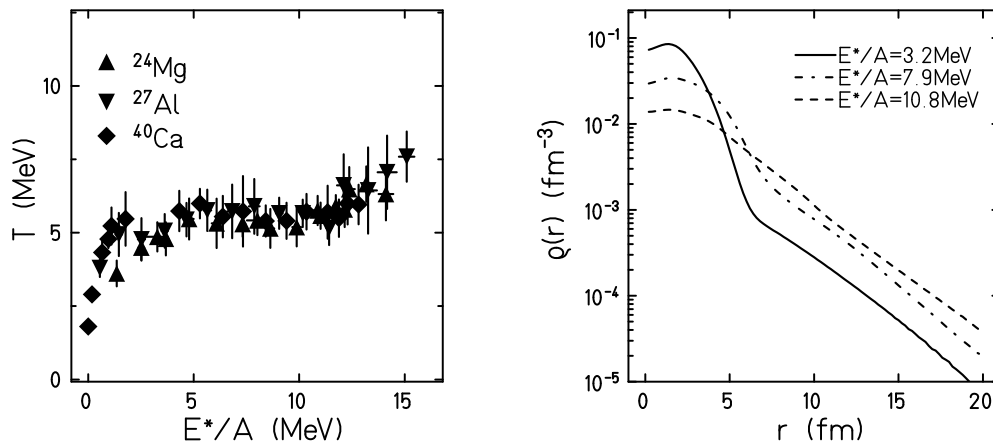


Figure 4. Results of FMD calculations: caloric curves of ^{24}Mg , ^{27}Al , and ^{40}Ca (left panel) and time-averaged radial density distributions of ^{24}Mg at various excitation energies in the coexistence region (right panel; from Ref. [49]).

temperature. As a remarkable result it was shown that the nuclear dynamics, as represented in these advanced transport-type models, generate a phase transition without any further assumptions.

Caloric curves obtained in the FMD study are shown in Fig. 4. The extracted temperatures exhibit a plateau that extends over about 8 MeV per nucleon of excitation energy and has its origin in the coexistence of liquid and nuclear phases in the system. The densities reflect the transition from a liquid phase in equilibrium with its surrounding vapor to the pure vapor phase. The properties of the system in these asymptotic states were identified as those of a Fermi liquid and a Fermi gas (Van-der-Waals gas in the AMD). Both groups have also demonstrated that the external conditions, the container which controls the pressure, have a strong influence on the properties of the transition. Changing the confinement gives the possibility to map out the phase diagram. The latent heat of the ^{16}O system approaches zero at $T \approx 10$ MeV which may be associated with the critical temperature for that system.

There is no external confinement in the real experiment, and the time scales of hot-fragmentation reactions are rather short. It is therefore even more surprising that the temperature-energy correlation measured for the breakup states exhibits such a similar behavior. The data for ^{197}Au fragmentation shown in Fig. 5 represent the results for 600 MeV per nucleon [51], with small modifications due to additional experimental information and corrections, and the results for 1000 MeV per nucleon obtained more recently [52]. The temperature of the transition region is close to that obtained with the dynamical [49] or statistical models [7,53,54] and does not change with the bombarding energy. In contrast to it, the energy associated with the spectator source increases by, on the average, 30% over the range 600 to 1000 MeV per nucleon, a behavior inconsistent with the universality of the spectator decay that so clearly appears in other variables [21]. It is caused by the energy dependence of the mean kinetic energies of nucleons in the spectator

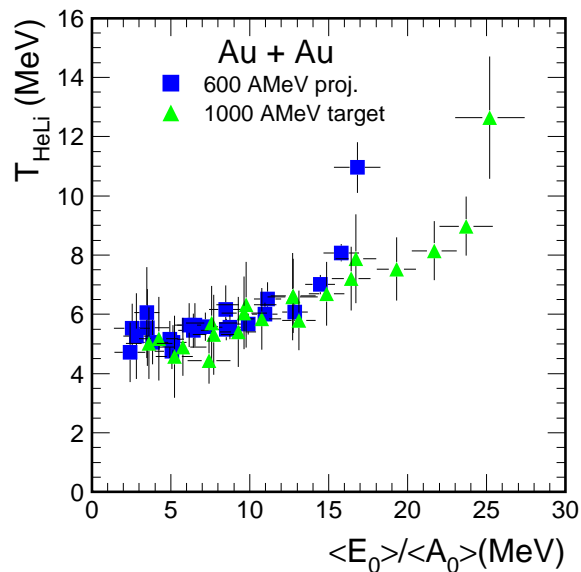


Figure 5. Caloric curve for spectator decays in ^{197}Au on ^{197}Au collisions. The temperatures were determined from helium and lithium isotope ratios of projectile fragments at 600 AMeV and of target fragments at 1000 AMeV (from Ref. [29]).

frame and most likely indicates that contributions from the early stages of the reaction have been included in the calorimetry for the spectator source. As a consequence, the apparent latent heat deduced even for the lower energy of 600 MeV per nucleon should be considered as an upper limit.

Breakup temperatures and energy contents of the fragmenting system were measured and correlated by several other groups for a variety of different reactions [25,55–58]. The basic methods were identical with some variation in the approximations that had to be made. Differences exist, e.g. in whether and how the effects of sequential decays on the temperature were taken into account, whether the neutron multiplicities and kinetic energies were measured or estimated, and whether and how preequilibrium components were identified and explicitly excluded. The last point is part of the bigger problem of identifying and properly selecting the fragmenting source which is crucial.

The resulting caloric curves have several features in common but are considerably different in detail. A deviation from the behavior of a Fermi liquid is observed for all reactions but at different temperatures between 5 and 7 MeV. The slopes are somewhat different and the upbend at high excitations is only seen in the ^{197}Au spectator decay (Fig. 5). It is not observed for the other reactions which, however, do not easily lead to comparable excitation energies (Fig. 3).

Apart from the experimental differences and imperfections, it is the transient nature of the reaction process which most likely prevents a single universal curve to emerge from these studies. To the extent that the equilibrated breakup state is an idealization, measured fragment yields represent integrals over finite emission times [58–60], with pre-

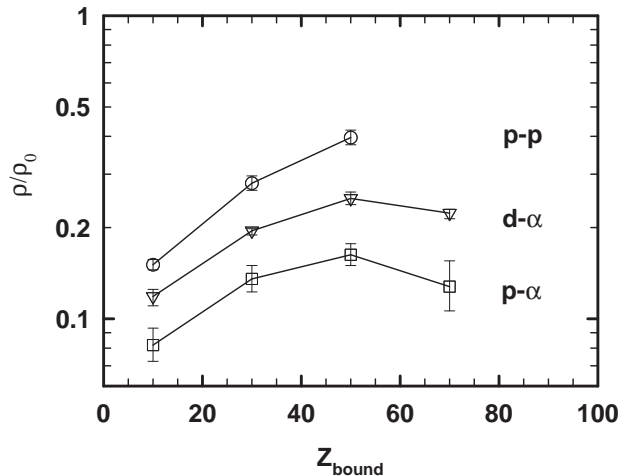


Figure 6. Breakup density ρ/ρ_0 as deduced from p-p, p- ^4He , and d- ^4He correlation functions measured for ^{197}Au on ^{197}Au reactions at 1000 AMeV. The rapid decrease of the density with decreasing Z_{bound} reflects the changing mass of the spectator source. Note the logarithmic ordinate scale (from Ref. [61]).

breakup and post-breakup contributions varying among different reactions. Furthermore, the expansion dynamics may generate transient pressures that are different for different types of hot-fragmentation reactions. The prominent role of the pressure, however, is known from the model experiments [49,50].

4. PARAMETERS OF THE BREAKUP STATE

Temperatures and excitation energies are only two of the quantities of interest that characterize the breakup states. Techniques for determining other breakup parameters have been successfully developed and applied. Among them, the density is of particular importance because an expansion to low density is a basic ingredient of the multifragmentation scenario.

Low densities in agreement with model expectations were recently reported for spectator decays following ^{197}Au on ^{197}Au reactions at 1000 MeV per nucleon [61]. They were deduced from measured correlation functions for proton pairs and for unlike pairs of protons or deuterons in coincidence with α particles. The correlation functions were found to exhibit the surprising property that their variation with Z_{bound} is rather small, indicating source extensions that do not change dramatically with impact parameter in these reactions. The observed variation of the density with impact parameter is mainly caused by the variation of the mass of the intermediate spectator system (Fig. 6).

Associated time scales were deduced from the same proton-proton data with the technique of directional analysis [62]. They are rather short, of the order of 20 fm/c, and comparable with the collision time in the entrance channel. While this may indicate that a majority of these protons, selected to have energies of $E \geq 20$ MeV in the spectator frame, may originate from early stages of the collision, it is still obvious that hot fragmen-

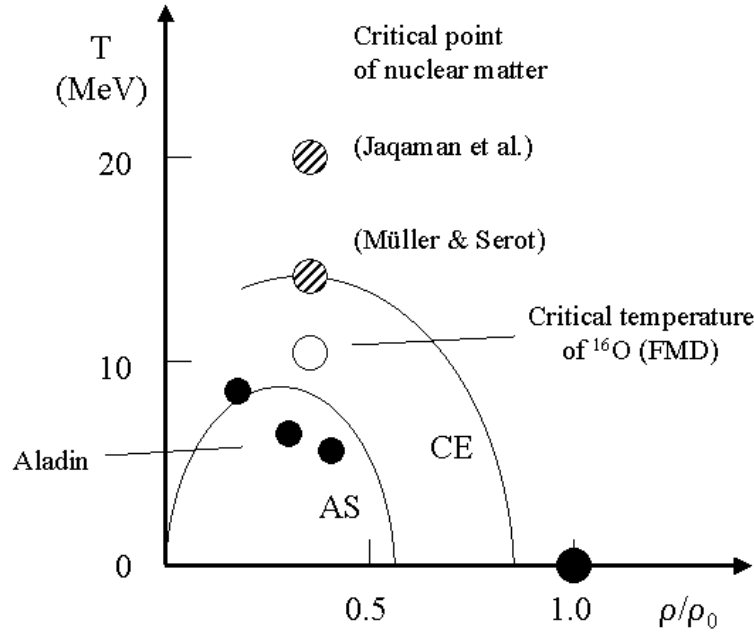


Figure 7. Temperature-versus-density diagram with the saturation point of nuclei (closed circle), critical points of nuclear matter (hatched, from Refs. [41,45]), the critical temperature of ^{16}O according to the FMD [49], and with experimental results (dots) obtained by correlating measured temperatures and densities. The coexistence line (CE) and the adiabatic spinodal (AS) for infinite matter, from Ref. [41], are indicated.

tation initiated by relativistic projectiles is a fast process. The emission times obtained from fragment-fragment correlations (Fig. 2) are larger by only a factor of two.

With experimental values for temperatures and densities at hand, the breakup conditions can be displayed in the temperature-versus-density plane, commonly used to characterize the nuclear phase behavior. The three data points (errors are omitted) shown in Fig. 7 are obtained by correlating the measured temperatures T_{HeLi} (Figs. 3 and 5) with the p-p densities of Fig. 6. The resulting trajectory in the phase diagram tends to higher temperatures and lower densities in the more violent collisions. It is important to note that this breakup (equilibrium) trajectory is practically orthogonal to the actual reaction trajectory followed by the system as it expands from higher to lower temperatures [63,64].

The measured breakup conditions are at comparable densities but at temperatures far below the critical point of nuclear matter as obtained in the calculations of Refs. [41,44,45]. They are also below the critical temperature obtained for the finite ^{16}O nucleus from the FMD experiment [49]. The conclusion that the breakup occurs in the coexistence region thus seems justified also from this perspective. Alternatively, it may be derived from the observation that multifragmentation populates the partition space predicted for the coexistence region by the statistical models.

The answer to the question what causes fragmentation is less obvious. As sketched in the figure, the experimental breakup points are barely inside the adiabatic spinodal of

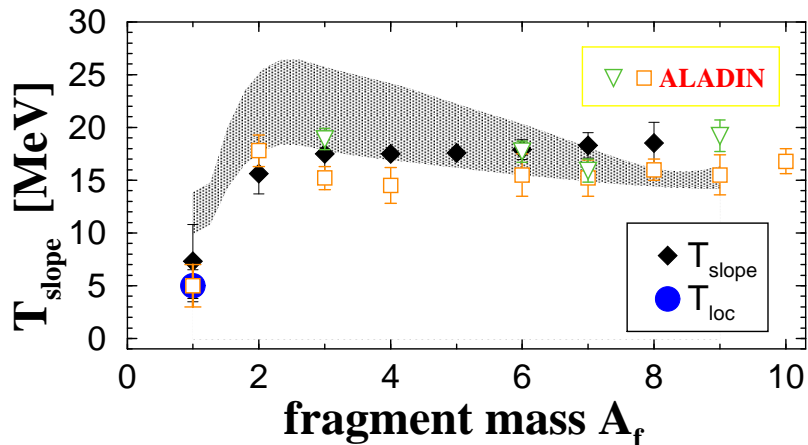


Figure 8. Comparison of experimental (open symbols, from Ref. [22]) and theoretical (closed diamonds) slope temperatures for spectator decays as a function of the fragment mass for spectator decays following ^{197}Au on ^{197}Au collisions. The local nucleon temperature $T_{\text{loc}} \approx 5$ MeV is indicated at $A_f = 1$, the shaded area represents the range of slope temperatures obtained by applying coalescence to a statistical nucleon distribution (from Ref. [68]).

the infinite system. In finite nuclei, this region of volume instability is probably limited to much lower temperatures. The expanding systems therefore seem to fragment before coming even close to it. Such a conclusion may appear speculative at present, but the need for systematic studies of the instabilities of finite nuclei is rather obvious [65–67]. Surface modes are an alternative to bulk instabilities. While they are expected to be slow in homogeneous systems [67], they may be rapidly excited during the early stages of the collision. Nuclear systems are predicted to be resilient to gentle surface excitations but not to major distortions following more violent encounters [13].

Additional insight in this direction may come from an improved understanding of the kinetic energy spectra of light particles and fragments. In cases of bulk fragmentation, the slope temperatures extracted from fragment spectra are inconsistent with the chemical temperatures obtained with the double-ratio method. However, for spectator decays at relativistic bombarding energies, it has been shown that these temperature values can be consistently understood if the slope temperatures are assumed to reflect the intrinsic Fermi motion, as assumed in the Goldhaber model [22]. Recent calculations with transport models, which incorporate Fermi motion, support this interpretation [9,68]. The energies of spectator fragments are well reproduced, and the coexistence of qualitatively different internal (or local) temperatures and fragment slope temperatures has been demonstrated (Fig. 8). The experimental and theoretical findings suggest that fragments are preformed at an early stage in these collisions (≤ 50 fm/c) before they may expand to typical breakup densities. To resolve this apparent contradiction to the filling of the phase space at breakup, the basis of the statistical approaches, is an interesting task for the future.

5. CONCLUDING REMARKS

There are many different ways for transforming cold into hot nuclear matter, and we have learned to exploit their different features in our efforts to understand the fragmentation processes. The question of how fragments are formed, the problem of identifying the dominant mechanisms, has been a recurrent theme during this talk. It continues to be a challenge, even though remarkable progress has been made within the last few years.

While this requires a realistic modelling of the dynamics, it does not reduce the statistical approaches in their role and importance. Not only is it demonstrated that the instabilities governing the fragmentation fill the phase space, but it is also the statistics and thermodynamics of the process that allow us to establish the connection to the nuclear phase transition.

The liquid-gas phase transition continues to act as a major motivation and has inspired wider investigations of phase transitions in small systems, extending beyond the nuclear domain. This more general approach seems extremely interesting and rewarding. The caloric curve of nuclei has been emphasized in this talk, but there are other potential observables, not necessarily less challenging on the experimental side, which will be discussed at this conference and should be further pursued and exploited in the future.

The uncertainties associated with the measurement of temperatures have been extensively investigated. The temperature differences seen with different methods have led to new insights into the fragmentation mechanism. Experimentally, the bigger challenge probably is the identification of the source and the measurement of its excitation energy at breakup. There will be limitations in how far we can go with the assumption of a well defined breakup configuration. The continuous evolution of the reaction and emission processes may not allow a precise distinction between the equilibrated emissions and those preceding it.

Finally, the majority of the data included here has come from elaborate experiments with approximately 4π coverage in the respective source frames. It is a pleasure to just look at such data, and it is gratifying to see the big investments in funds and manpower being justified. Moreover, it provides encouragement for those who are presently designing or completing potentially even more powerful detection devices for future research.

Illuminating and inspiring discussions with my colleagues at the GSI, notably A.S. Botvina, H. Feldmeier, U. Lynen, W.F.J. Müller, W. Nörenberg, W. Reisdorf and C. Schwarz are gratefully acknowledged. In addition, I like to thank L. Beaulieu, D. Durand, T. Gai-tanos, J. Łukasik, K.H. Schmidt and V.E. Viola for providing me with graphics for the talk and for this manuscript.

REFERENCES

1. J.P. Bondorf, D. Idier, and I.N. Mishustin, *Phys. Lett. B* 359 (1995) 261.
2. L.G. Moretto and G.J. Wozniak, *Ann. Rev. Nucl. Part. Science* 43 (1993) 379.
3. For a recent review of the field see, e.g., *Proceedings of the International Workshop XXVII on Gross Properties of Nuclei and Nuclear Excitations*, Hirschegg, Austria, edited by H. Feldmeier et al. (GSI, Darmstadt, 1999).
4. while this manuscript was being prepared two new review articles have become avail-

- able: J. Richert and P. Wagner, nucl-th/0009023; S. Das Gupta, A.Z. Mekjian, and M.B. Tsang, nucl-th/0009033.
5. D.H.E. Gross, Rep. Prog. Phys. 53 (1990) 605.
 6. J.P. Bondorf et al., Phys. Rep. 257 (1995) 133.
 7. Al.H. Raduta and Ad.R. Raduta, Phys. Rev. C 61 (2000) 034611.
 8. H.W. Barz et al., Phys. Lett. B 382 (1996) 343.
 9. P.B. Gossiaux et al., Nucl. Phys. A 619 (1997) 379.
 10. A. Ono, Phys. Rev. C 59 (1999) 853.
 11. C. Fuchs et al., Nucl. Phys. A 626 (1997) 987.
 12. J. Nemeth et al., Z. Phys. A 323 (1986) 419.
 13. M. Colonna, J. Cugnon, and E.C. Pollacco, Phys. Rev. C 55 (1997) 1404.
 14. T. Lefort et al., Phys. Rev. Lett. 83 (1999) 4033.
 15. L. Beaulieu et al., Phys. Lett. B 463 (1999) 159.
 16. L. Beaulieu et al., Phys. Rev. Lett. 84 (2000) 5971.
 17. D. Durand, Nucl. Phys. A 630 (1998) 52c.
 18. U. Jahnke et al., Phys. Rev. Lett. 83 (1999) 4959.
 19. Rulin Sun et al., Phys. Rev. Lett. 84 (2000) 43.
 20. E.C. Pollacco et al., Phys. Lett. B 482 (2000) 349.
 21. A. Schüttauf et al., Nucl. Phys. A 607 (1996) 457.
 22. T. Odeh et al., Phys. Rev. Lett. 84 (2000) 4557.
 23. S.P. Avdeyev et al., Eur. Phys. J. A 3 (1998) 75.
 24. V.A. Karnaukhov et al., Phys. of Atomic Nuclei 62 (1999) 237.
 25. J.A. Hauger et al., Phys. Rev. C 57 (1998) 764.
 26. A. Insolia et al., Phys. Rev. C 61 (2000) 044902.
 27. J.A. Hauger et al., Phys. Rev. C 62 (2000) 024616.
 28. K.H. Tanaka et al., Nucl. Phys. A 583 (1995) 581.
 29. T. Odeh, Ph.D. thesis, Universität Frankfurt, 1999.
 30. M.L. Cherry et al., Phys. Rev. C 52 (1995) 2652.
 31. W. Reisdorf and H.G. Ritter, Ann. Rev. Nucl. Part. Science 47 (1997) 663.
 32. T.A. Armstrong et al., Phys. Rev. Lett. 83 (1999) 5431.
 33. G.J. Kunde et al., Phys. Rev. Lett. 74 (1995) 38.
 34. S. Chikazumi et al., Phys. Lett. B 476 (2000) 273.
 35. R. Nebauer and J. Aichelin, Nucl. Phys. A 650 (1999) 65.
 36. M. D'Agostino et al., Phys. Lett. B 371 (1996) 175.
 37. M.F. Rivet et al., Phys. Lett. B 430 (1998) 217.
 38. J. Lukasik et al., Phys. Rev. C 55 (1997) 1906.
 39. J.F. Dempsey et al., Phys. Rev. C 54 (1996) 1710.
 40. E. Plagnol et al., Phys. Rev. C 61 (2000) 014606.
 41. H. Müller and B.D. Serot, Phys. Rev. C 52 (1995) 2072.
 42. Ph. Chomaz and F. Gulminelli, Phys. Lett. B 447 (1999) 221.
 43. H.S. Xu et al., Phys. Rev. Lett. 85 (2000) 716.
 44. G. Sauer, H. Chandra, and U. Mosel, Nucl. Phys. A 264 (1976) 221.
 45. H. Jaqaman, A.Z. Mekjian, and L. Zamick, Phys. Rev. C 27 (1983) 2782.
 46. X. Campi, Phys. Lett. B 208 (1988) 351.
 47. S. Das Gupta and A.Z. Mekjian, Phys. Rev. C 57 (1998) 1361.

48. D.H.E. Gross, Phys. Rep. 279 (1997) 119.
49. J. Schnack and H. Feldmeier, Phys. Lett. B 409 (1997) 6.
50. Y. Sugawa and H. Horiuchi, Phys. Rev. C 60 (1999) 064607.
51. J. Pochodzalla et al., Phys. Rev. Lett. 75 (1995) 1040.
52. W.F.J. Müller et al., in Ref. [3], p. 200.
53. H. Xi et al., Z. Phys. A 359 (1997) 397; Eur. Phys. J. A 1 (1998) 235.
54. J.P. Bondorf, A.S. Botvina, and I.N. Mishustin, Phys. Rev. C 58 (1998) R27.
55. Y.-G. Ma et al., Phys. Lett. B 390 (1997) 41.
56. K. Kwiatkowski et al., Phys. Lett. B 423 (1998) 21.
57. M. D'Agostino et al., Nucl. Phys. A 650 (1999) 329.
58. J. Cibor et al., Phys. Lett. B 473 (2000) 29; K. Hagel et al., Phys. Rev. C 62 (2000) 034607.
59. H. Xi et al., Phys. Rev. C 57 (1998) R462.
60. V.E. Viola, K. Kwiatkowski, and W.A. Friedman, Phys. Rev. C 59 (1999) 2660.
61. S. Fritz et al., Phys. Lett. B 461 (1999) 315.
62. C. Schwarz et al., Proceedings of 3rd Catania Relativistic Ion Studies, Phase Transitions in Strong Interactions: Status and Perspectives (CRIS 2000).
63. W.A. Friedman, Phys. Rev. C 42 (1990) 667.
64. G. Papp and W. Nörenberg, APH Heavy Ion Physics 1 (1995) 241.
65. C.J. Pethick and D.G. Ravenhall, Nucl. Phys. A 471 (1987) 19c.
66. M. Colonna, Ph. Chomaz, and A. Guarnera, Nucl. Phys. A 613 (1997) 165.
67. W. Nörenberg, G. Papp, and P. Rozmej, preprint nucl-ex/0009002, subm. to Eur. Phys. J. A (2000).
68. T. Gaitanos, H.H. Wolter, and C. Fuchs, Phys. Lett. B 478 (2000) 79.